PCCP

Accepted Manuscript

ROYAL SOCIETY OF CHEMISTRY

www.rsc.org/pccp

Isotopic Studies of the Ammonia Decomposition Reaction Mediated by Sodium Amide

Thomas J. Wood[†], Joshua W. Makepeace[†‡], Hazel M. A. Hunter[†], Martin O. Jones[†] and William I. F. David[†‡]*

[†] ISIS Facility, Rutherford Appleton Laboratory, Harwell Oxford, Didcot, OX11 0QX, UK

[‡] Inorganic Chemistry Laboratory, University of Oxford, Oxford, OX1 3QR, UK

*Corresponding author: bill.david@stfc.ac.uk

ABSTRACT

We demonstrate that the ammonia decomposition reaction catalysed by sodium amide proceeds under a different mechanism to ammonia decomposition over transition metal catalysts. Isotopic variants of ammonia and sodium amide reveal a significant kinetic isotope effect in contrast to the nickel-catalysed reaction where there is no such effect. The bulk composition of the catalyst is also shown to affect the kinetics of the ammonia decomposition reaction.

INTRODUCTION

Ammonia offers excellent properties as an energy vector for a future carbon-free economy as it is liquid at room temperature and moderate pressure (10 bar) and under those conditions has among the highest volumetric and gravimetric hydrogen densities known (121 kg H_2 m^{-3} and 17.8 wt% respectively).[1,2] This compares favourably to storing hydrogen in its elemental form where liquefaction (below 33 K) or high pressures (700 bar) give lower hydrogen densities than ammonia itself. Lightweight solid state hydrogen stores have similar hydrogen densities to ammonia, but suffer from issues of reversibility and require high temperatures to release the hydrogen.[3,4]

Recently we showed that sodium amide may be used as a catalyst to effectively decompose ammonia into its constituent elements, nitrogen and hydrogen, with similar performance to the state-of-the-art ruthenium catalysts but at a fraction of the cost.[5] This catalytic activity was proposed to be due to a combination of the following two reactions:

$$Na + NH_3 \rightarrow NaNH_2 + \tfrac{1}{2}H_2 \qquad (1)$$

$$NaNH_2 \rightarrow Na + \tfrac{1}{2}N_2 + H_2 \qquad (2)$$

whereby it may be seen that, under flowing conditions, ammonia can be decomposed continuously into nitrogen and hydrogen (a phenomenon recognised as early as 1894).[6]

Traditionally, transition metal catalysts have been used for the decomposition of ammonia with the relative activities being closely related to those for the reverse reaction of ammonia formation.[7,8] As such, iron and ruthenium are the most commonly used catalysts.[9,10] The mechanism for these reactions follows a standard heterogeneous catalytic pathway with ammonia adsorbed onto the catalyst surface, followed by breaking of the N-H bonds to give adsorbed nitrogen and hydrogen atomic species which then desorb as N_2 and H_2. Extensive studies have been performed under different conditions to elucidate the reaction mechanism.[11,12] In general, these have shown that the rate-limiting step is the desorption of nitrogen from the metal surface, *i.e.* the formation of the nitrogen-nitrogen triple bond (although there is some variation depending on the conditions and transition metal used).[13,14,15,16,17] Alkali and alkaline earth metals have been used to promote the surface catalytic activity of ruthenium and iron and therefore lower the temperatures required.[18,19,20,21,22,23] The question arises as to whether the activity of sodium amide falls into this category of promoting the catalytic activity of a transition metal *via* surface interaction, or whether the ammonia decomposition proceeds independently of the transition metal *via* the sodium amide decomposition and formation reactions proposed above.

In this paper, we use different isotopologues of ammonia and sodium amide (NH_3, ND_3, $NaNH_2$ and $NaND_2$) to study the ammonia decomposition reaction *via* mass spectrometry analysis of the isotope traces, in order to elucidate the nature of the reaction, including its mechanism and possible rate-limiting steps.

EXPERIMENTAL

Ammonia decomposition experiments with different isotopes were performed in a nickel-plated stainless steel reactor with an internal volume of 21.3 cm^3. As described previously,[5,24] the reactor was fitted with an inlet gas pipe running from the reactor lid to around 1 cm from the base of the reactor. A thermocouple monitored the temperature around 5 mm from the bottom of the reactor. Gas flows (NH_3 and ND_3) were mediated by mass flow controllers (HFC-302, Teledyne Hastings Instruments) and the outlet gas flow monitored by a mass flow meter (HFM-300, Teledyne Hastings Instruments) in a custom-designed gas panel, Figure 1. The gas species flowing out from the reactor were characterised by Quantitative Gas Analysis (QGA) using a Hiden Analytical HPR-20 QIC R&D mass spectrometer system in histogram mode (MASsoft 7), monitoring peaks from m/z = 1 to m/z = 40 (inclusive). The post-reaction gas species were also flowed through an infrared gas cell (Specac) with a path length of 10 cm contained within a Bruker Vertex 80v spectrometer (equipped with a liquid-nitrogen cooled mercury-cadmium-telluride detector) with spectra recorded every 30 s from 5500–600 cm^{-1} for the duration of the experiment (using Bruker OPUS 7.2 software).

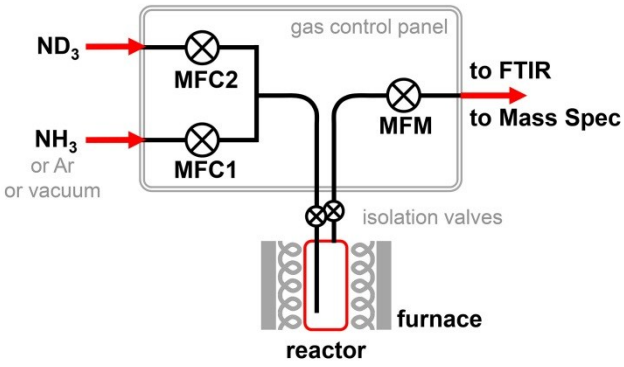

Figure 1: Experimental gas handling setup, where the inlet NH_3 or ND_3 gas flows (or vacuum) are controlled by mass flow controllers (MFCs) prior to the reactor. Valves are located above the reactor inlet and outlet, allowing it to be isolated when evacuating the gas panel upstream. Gas flow out of the reactor is monitored by a mass flow meter (MFM) before analysis *via* a mass spectrometer and Fourier-transform infrared (FTIR) spectrometer.

The isotopic reactions used the following gases: NH_3 (99.999%, SIP Analytical), ND_3 (99 atom % D, Sigma-Aldrich) and argon (99.998%, BOC). Isotopic experiments were performed by loading 0.1 g of the powder into the reactor under an argon atmosphere. Sodium amide ($NaNH_2$, hydrogen storage grade, Sigma-Aldrich) and its deuterated isotopologue ($NaND_2$), which was synthesised from passing ND_3 gas over $NaNH_2$ for 3 h at 300 °C, were used. For the latter, the complete exchange of hydrogen for deuterium was confirmed by Raman microscopy (see ESI).

Three types of isotope exchange experiment were undertaken for the ammonia decomposition:

1) Without a catalyst (blank) under a flow of NH_3, switching to a flow of ND_3 (with residual NH_3 in the reactor) and finally switching back to a flow of NH_3 (with residual ND_3 in the reactor). The use of the term “blank” throughout this article denotes no catalyst powder is present in the reactor.
2) With a catalyst ($NaNH_2$) under a flow of NH_3, switching to a flow of ND_3.
3) With a catalyst ($NaND_2$) under a flow of ND_3, switching to a flow of NH_3.

Samples were heated up to a temperature of around 200 °C at 5 °C min^{-1} under flowing argon, which was used as the infrared background spectrum. The gas flow was then changed to NH_3 or ND_3 and the reactor heated to 485 °C at 5 °C min^{-1}. Typically the flow of gas was 25 sccm into the reactor and upon switching gas, the gas panel was evacuated up to the reactor inlet (in order to minimise NH_3/ND_3 mixing) and then the relevant isotopologue was introduced also at 25 sccm.

Additionally two experiments examined the decomposition of $NaNH_2$ or $NaND_2$ under flowing argon gas. To perform these experiments 0.2 g of catalyst sample was introduced into the reactor with 15

sccm of flowing Ar (without infrared monitoring). The furnace was heated at a rate of 5 °C min^{-1} up to a temperature of 550 °C and the mass spectrometry output was measured throughout.

Mass spectrometry data analysis involved fitting each histogram collected to fractions of the following gases: Ar, N_2, ND_3, ND_2H, NDH_2, NH_3, D_2, HD and H_2. The ammonia species were assumed to have statistically scrambled hydrogen/deuterium (since this occurs at room temperature), therefore seven parameters were used: the gas fractions of Ar, N_2, ammonia species, D_2, HD and H_2 and the deuteration fraction of ammonia. The gas fraction of the ammonia species is calculated as the sum of the fractions of NH_3, NDH_2, ND_2H and ND_3, given the shorthand "NH_3+ND_3", whereas the deuteration fraction is calculated as $(⅓NDH_2 + ⅔ND_2H + ND_3)/(NH_3 + NDH_2 + ND_2H + ND_3)$, which is given the shorthand "$ND_3/(NH_3+ND_3)$". For experiments where very little argon was expected, the fraction of argon parameter was set to zero and not fitted. The mass spectrometer was calibrated using pure gas streams of the relevant gases (Ar, N_2, ND_3, NH_3, D_2 and H_2), in order to ascertain the fragment peak ratios, Table S1. The relative ionization factors (how well the mass spectrometer filament ionizes each gas) were calculated from running 50/50 mixtures of each gas with argon (which itself was given a standardized ionization factor of 1.0). For hydrogen and deuterium, these values were internally calibrated during each experiment if possible. The fragmentation patterns and ionization factors of the partially deuterated species were interpolated from the values of the purely hydrogenated and wholly deuterated isotopologues (NH_3, ND_3, H_2, D_2). Further details are available in the ESI.

Fourier-transform infrared data analysis entailed the monitoring of the N-H stretching rovibrational peaks between 4600 and 4150 cm^{-1} and the N-D stretching rovibrational peaks between 2750 and 2200 cm^{-1}, Figure S2. After the background spectrum was subtracted from the measured spectrum, the area of these peaks was calculated and divided by the areas measured for the pure ND_3 and NH_3 calibration runs to obtain estimates of ND_3 and NH_3 partial pressures. Unlike mass spectrometry, gas-phase infrared spectra were subject to systematic errors from water peaks with varying intensities in the background. When the system was operating under low flow, there was also the potential for ambient air to enter into the gas cell. As a result of these errors being difficult to quantify, the mass spectrometry data are the primary basis for discussion through the remainder of the paper. Nevertheless, the gas-phase infrared data are in qualitative agreement and are presented in Figures S3–S5.

RESULTS AND DISCUSSION

Kinetic Isotope Effects

Kinetic isotope effects were calculated from the ratio of the rate constants for the H-containing reaction and the D-containing reaction (k_H and k_D). The variation of rate constant with conversion at a given temperature was calculated from data previously gathered under variable flow conditions.[5] Rates were assumed to follow the relationship:

$$r = k[NH_3]^a \quad (3)$$

where *r* is the rate, *k* the rate constant and *a* the pseudo-order of reaction.[a] It should be noted that this approximation is valid only when the reaction lies at some point between the two extremes of pure NH_3 or $½N_2 + {}^3/_2H_2$ (as per the ammonia decomposition reaction). Since the gas introduced in all our experiments is pure, undiluted ammonia this assumption holds. There is also a second assumption, that the reaction mechanism does not change whether the reactant is hydrogenated or deuterated, which is equivalent to the transition state(s) for the rate-limiting step(s) of the reaction being structurally unchanged (except for substitution of hydrogen with deuterium atoms or vice versa). This second assumption underlies the significance of kinetic isotope effects and is presumed to be true in this reaction.[25] Given that the rate is also calculable from the following expression:

$$r = -\frac{d[NH_3]}{dt} \quad (4)$$

We can substitute for *r* (equation (3) into (4)) to get the following differential equation:

$$\frac{d[NH_3]}{[NH_3]^a} = -kdt \quad (5)$$

This gives the solution:

$$[NH_3] = (1 - (1 - a)kt)^{\frac{1}{1-a}} \quad (6)$$

Equation (6) was fitted to the experimental data for constant temperature, variable flow (15–100 sccm) NH_3 experiments using the blank reactor and the reactor with $NaNH_2$, Figure 2. These fits give values for *a* of 5.4(4) for the blank reactor and 1.56(9) for $NaNH_2$.

[a] It is important to clarify that the absolute values of *k* and *a* hold no significance with regards to the order of the reaction or providing any mechanistic insight. They can only be interpreted relatively.

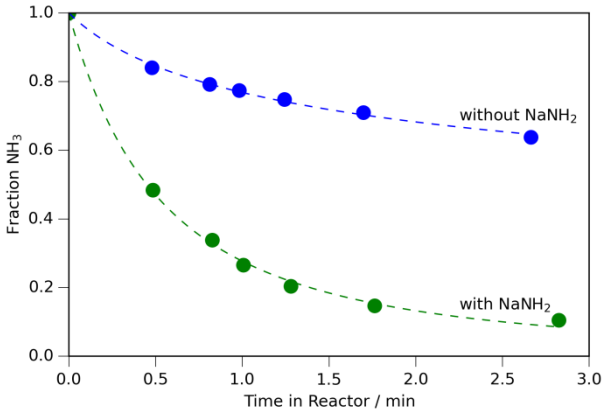

Figure 2: Plot of the decrease in fraction of NH_3 versus residence time in the reactor for the blank reactor and $NaNH_2$ (fits are the dashed lines).

Values obtained for the equilibrium fraction of ammonia can then be substituted into equation (6) along with the relevant value of *a* depending on the conditions of the experiment and the residence time in the reactor (which equals the reactor volume multiplied by the flow rate) to give pseudo-rate constant values for *k* for both the hydrogenated and deuterated experiments (k_H and k_D). This assumes that *a* is unchanged between hydrogenated and deuterated samples, which is equivalent to the assumption that the reaction mechanism and the rate-limiting step are unchanged.

The mass spectrometry data for the blank experiment (nickel-plated reactor without catalyst powder) are shown in Figure 3. From these data, it can be observed that the "NH_3 + ND_3" fraction is 0.577(7) under NH_3, rises initially upon introduction under ND_3 but then slowly equilibrates reaching 0.596(6). Switching back to NH_3 causes a small fall in the ammonia fraction. As the ammonia fraction reflects the rate of ammonia decomposition, this difference in ammonia fractions can be expressed as a kinetic isotope effect. For the blank reactor this equates to a kinetic isotope effect (k_H/k_D) of 1.10(8) once small systematic offsets with the mass flow controllers are taken into account. This is consistent with either a secondary kinetic isotope effect or no significant kinetic isotope effect, with steady-state conditions under NH_3 and ND_3 giving approximately the same ammonia conversion value.

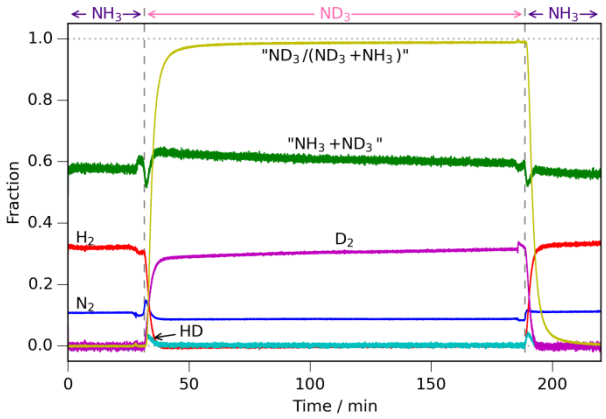

Figure 3: Mass spectrometry fractions for the blank reactor run under 25 sccm NH_3 (0–32 min and 189–220 min) or ND_3 (18–189 min), T = 494 °C.

Within the mass spectrometry data for the blank reactor, it can be seen that there exists a small fraction of HD, which is far less than would be expected from a statistical distribution of hydrogen species. This can be attributed to minimal mixing of NH_3 and ND_3 within the reactor during switchover. It is noted that the "$ND_3/(NH_3+ND_3)$" fraction rises on a slightly slower timescale than the D_2 signal, which indicates that the ammonia is not sticking to the walls of the reactor for long time periods (as observed under room temperature conditions).

The mass spectrometry data for the same experiment but with 0.1 g of $NaNH_2$ in the reactor are shown in Figure 4(a). The most noticeable difference is the large increase in conversion relative to the blank reactor as evidenced by the decrease in the "NH_3+ND_3" fraction. There is also a significant kinetic isotope effect observed both with the "NH_3+ND_3" fraction increasing from 0.060(1) to 0.125(1) moving from NH_3 to ND_3 flow.

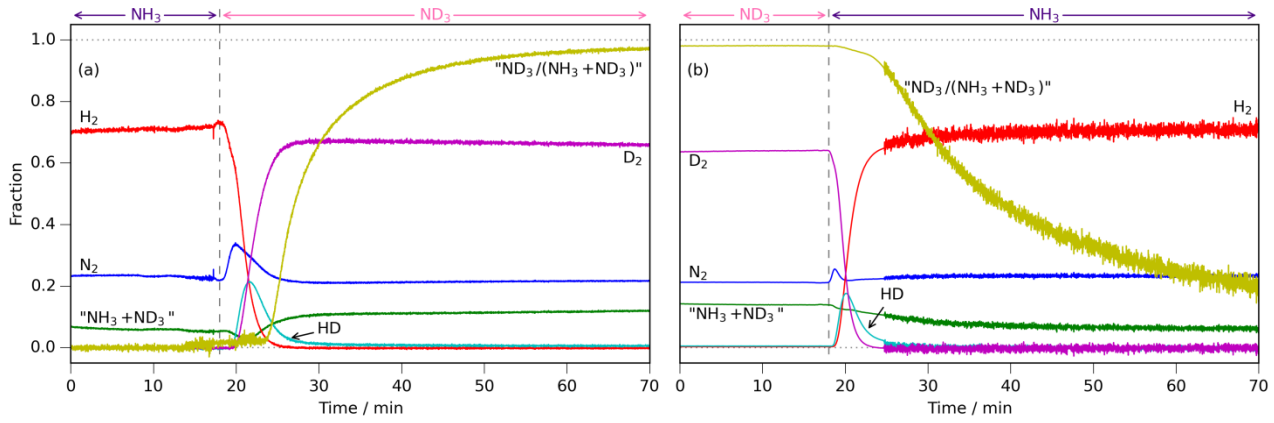

Figure 4: Mass spectrometry fractions for (a) 0.1 g $NaNH_2$ run under 25 sccm NH_3 (0–18 min) and subsequently under 25 sccm ND_3, T = 485 °C and (b) 0.1 g $NaND_2$ run under 25 sccm ND_3 (0–18 min) and subsequently 25 sccm NH_3, T = 485 °C.

This kinetic isotope effect is also observed in the reverse reaction starting with $NaND_2$ under ND_3 and switching to NH_3, Figure 4(b). The fraction of ammonia according to the mass spectrometry under ND_3 is 0.1393(2) and decreases to 0.057(4) under NH_3. Once mass flow offsets are taken into account, the combination of both $NaNH_2$ + ND_3 and $NaND_2$ + NH_3 experiments gives a kinetic isotope effect of 1.77(11). The magnitude of this kinetic isotope effect shows that it is primary in origin (rather than secondary, which would have a maximum of 1.4), which indicates that a bond including at least one hydrogen (or deuterium) atom is broken or formed in the rate-limiting step.

Primary kinetic isotope effects are observed because of differences in the zero point energy of the reactants, with deuterium bonds sitting lower in energy than their hydrogen counterparts. This difference in zero point energy decreases in the transition state of the reactants (the momentary structure at the maximum of the reaction coordinate energy), which overall results in a lower activation energy for the breaking/forming of hydrogen bonds compared to deuterium bonds and a concomitant difference in reaction rates (for the rate-limiting step).

Given that there is no appreciable kinetic isotope effect observed in the blank reactor (k_H/k_D = 1.10(8)), it can be inferred that the rate-limiting step in this reaction is the desorption of nitrogen gas from the surface of the nickel (*i.e.* N≡N bond formation), since this is the only step in the ammonia decomposition reaction which does not involve either the breaking of an N-H bond or the formation of an H-H bond, both of which would be expected to show primary kinetic isotope effects (in this system the formation of an H-H bond would be expected from combination of chemisorbed hydrogen atoms and therefore would show a kinetic isotope effect). By contrast, the significant kinetic isotope effect observed in the case of the sodium amide catalyst (k_H/k_D = 1.77(11)) shows that the rate-limiting step involves either N-H bond scission or H-H bond formation.

Although the difference in kinetic isotope effect with and without sodium amide implies that the sodium amide case proceeds *via* a different mechanism, there is also the possibility of sodium promoting nickel-mediated ammonia decomposition. Metal catalyst promoters have several modes of action including structural promotion (where the solid state chemistry of the catalyst is modified) and bifunctional promotion where the promoter plays a chemical role in the catalytic event.[26] For alkali metals in ammonia decomposition, the promotion effect is probably due to electron transfer between the alkali metal and the catalyst surface, as is the case for ammonia synthesis.[27] The possibility of the observed kinetic isotope effects being solely due to promoting action is unlikely however, since, according to Tamaru,[13] the kinetics of ammonia decomposition over transition metals can be generalized into two limiting cases. The first is where chemisorbed nitrogen is easily rehydrogenated to form ammonia (*i.e.* the reverse reaction rate constant for the N-H bond scissions

on the nickel surface is large) and the second is where chemisorbed nitrogen is mostly desorbed before it is rehydrogenated. In the former case, the nitrogen desorption is the rate-limiting step and there is no observable kinetic isotope effect. In the latter case, the nitrogen desorption is relatively fast, and therefore there is a kinetic isotope effect seen. The rate-limiting step changes under varying conditions with the former seen, in general, at lower temperatures and higher hydrogen pressures, and the latter at higher temperatures and lower hydrogen pressures. The only difference in conditions between the blank reactor and the sodium amide experiments (other than the presence of the sodium amide) is that there is increased conversion, leading to a higher partial pressure of hydrogen. In this scenario, therefore, the higher partial hydrogen pressure will increase the rate of ammonia re-formation on the nickel walls, which would mean that the nitrogen desorption would most likely still be the rate-limiting step. When sodium amide is present, given that the opposite effect is observed (*i.e.* there is a significant kinetic isotope effect of 1.77(11)), it is reasonable to infer that the sodium amide decomposes ammonia independently of the nickel-plated reactor and that any promotion effect of the sodium is minimal (indeed, the increased hydrogen partial pressure as a result of the sodium amide decomposition will suppress the nickel-mediated decomposition, since it favours the re-formation of ammonia). This conclusion is supported by previous studies on the effects of alkali metal promoters for ammonia decomposition on iron where nitrogen desorption is shown to remain the rate-limiting step.[28,29,30]

Mechanism and Rate-limiting Step

The presence of a kinetic isotope effect for the sodium amide-mediated decomposition (k_H/k_D = 1.77(11)) signifies that either an N-H bond is broken or an H-H bond is formed in the rate-limiting step:

$$2Na + 2NH_3 \rightarrow 2NaNH_2 + H_2 \qquad (8)$$

$$2NaNH_2 \rightarrow 2Na + N_2 + 2H_2 \qquad (9)$$

The formation of sodium amide, equation (8), entails the scission of two N-H bonds and the formation of one H-H bond. In equation (9) there are four N-H bonds broken and two H-H bonds and one N≡N bond formed. The presence of a significant kinetic isotope effect indicates that the N≡N bond formation is not the rate-limiting step.

An indication of which reaction includes the rate-limiting step may be ascertained by calculating whether the sodium amide exists as mostly sodium metal or sodium amide in the reactor under ammonia decomposition conditions, as this will give an indication of the relative ratio of the rate constants for the sodium amide formation and decomposition reactions. This may be ascertained by

calculating the volumes of the various gas species after NH_3 is switched for ND_3 (or vice versa). At the point of gas switchover from NH_3 to ND_3, any H-containing species detected in the mass spectra must be as a result of residual gas within the reactor or as a result of being released from the sodium amide ($NaNH_2$) sample. These volumes may be then compared with those ascertained for the blank reactor to remove the residual gas within the reactor component. For each experiment in Figures 3 and 4, the moles equivalent of H_2 or D_2 have been calculated from the mass spectrometry data by using the following expressions:

$$V_{H_2} = \left[\frac{3}{2}\int_0^t f_{am}(1 - D_{am})dt + \int_0^t f_{H_2}dt + \frac{1}{2}\int_0^t f_{HD}dt\right]F \qquad (10)$$

$$V_{D_2} = \left[\frac{3}{2}\int_0^t f_{am}D_{am}dt + \int_0^t f_{D_2}dt + \frac{1}{2}\int_0^t f_{HD}dt\right]F \qquad (11)$$

where V_i is the volume of i, f_{am} the fraction of all ammonia isotopologues ("NH_3+ND_3"), D_{am} the deuteration fraction of the ammonia species ("ND_3/(NH_3+ND_3)"), F the gas flow out of the reactor, t=0 is the time when the gas is switched over and t=t the time once equilibration has been reached. The volume is converted to moles, n, using the ideal gas equation n = pV/RT, and the results are shown in Table 1. Once the value for the blank reactor, which refers to any residual gas left in the reactor and the rig up to the mass spectrometer, has been taken into account then the amount of moles equivalent of H_2 produced from the $NaNH_2$ (once the gas input has been changed from NH_3 to ND_3) is approximately zero, which indicates that the sodium amide exists mostly as sodium metal and not $NaNH_2$. This implies that the formation of sodium amide from sodium metal and ammonia includes the rate-limiting step. In contrast, however, the amount of moles equivalent of D_2 produced from the $NaND_2$ (after switchover from ND_3 to NH_3) is greater than that expected if the equilibrium was 100% amide. This extra deuterium is attributed to ND_3 adsorbed on the amide surface or dissolved within the amide (which exists as liquid at these conditions). This indicates that for the deuterated isotopologue, the decomposition of sodium amide now includes the rate-limiting step, since the sodium amide exists mostly as $NaND_2$ not sodium metal. This is consistent with what might be expected, since the only difference in the reaction conditions is that there is a higher partial pressure of ammonia for the $NaND_2$ experiment (thanks to the kinetic isotope effect), which leads to the formation of amide being favoured while a lower partial ammonia pressure favours the amide decomposition.

Table 1: Volumes of gases produced and overall moles of H or D produced after gas switchover along with the moles of H or D in the original catalyst. It should be noted that the "NH_3" and "ND_3" volumes incorporate the relevant fractional components of NDH_2 and ND_2H.

	Volume / mL	**Gas produced / 10^{-3} mol**	**Catalyst / 10^{-3} mol equivalent**

Experiment	"NH_3"	H_2	HD	D_2	"ND_3"	equivalent[a] H_2	equivalent[a] D_2	H_2	D_2
$NaNH_2$ + ND_3	28.7(2)	82.3(5)	24.8(1)			-0.2(1)		2.584(3)	
$NaND_2$ + NH_3			17.2(1)	66.5(4)	77.6(5)		3.2(1)		2.373(2)

[a]After the blank reactor volumes have been taken into account.

A closer look at Figure 4 yields further observations that are consistent with the above analysis. In the $NaNH_2$ experiment (Figure 4(a)), after switchover to ND_3, there is an immediate dip in the fraction of ammonia ("NH_3 + ND_3") and a subsequent delay in the increase of the deuteration fraction of that ammonia ("$ND_3/(NH_3+ND_3)$") when compared to the $NaND_2$ experiment. This can also be seen in a much larger rise in the N_2 fraction for the $NaNH_2$ experiment. This is consistent with ND_3 reacting with elemental sodium in the reactor and the sodium/sodium amide equilibrium moving towards the amide. With $NaND_2$ (Figure 4(b)) after the introduction of NH_3, there is no delay in the decrease of "$ND_3/(NH_3+ND_3)$" fraction and no significant, immediate reduction in the "NH_3+ND_3"fraction itself. From these data, it can be concluded that both the decomposition and the formation of sodium amide (depending on the conditions) are important in the kinetics of ammonia decomposition.

These conclusions are consistent with the thermodynamics of the sodium amide formation and decomposition reactions. The changes in entropy (ΔS) for equations (8) and (9) (the formation and decomposition of sodium amide) are -101.9 J mol^{-1} K^{-1} and +200.9 J mol^{-1} K^{-1} respectively, which results in the formation of sodium amide becoming less favourable and the decomposition of sodium amide becoming more favourable as the temperature increases. At the temperature at which the ammonia decomposition was carried out in this study (485 °C), an equilibrium between sodium metal and sodium amide is likely to be thermodynamically feasible and the ratio of sodium metal to amide is determined by kinetics.

In contrast to the marked kinetic isotope effects observed under flowing ammonia (k_H/k_D = 1.77(11)), the mass spectrometry data for the decompositions of $NaNH_2$ and $NaND_2$ under flowing argon show no significant kinetic isotope effect, Figure 5. The H_2 peak and D_2 peak maxima are at 480 °C and 474 °C respectively, which is within the expected experimental uncertainty for this setup. A significantly increased temperature of decomposition for the $NaNH_2$ case would imply a secondary kinetic isotope effect where deuterium-containing bonds break and form faster than their hydrogen-containing counterparts. This would seem unlikely as secondary effects are usually due to stabilising contributions of β hydrogens/deuteriums, which are not obviously present in this system.

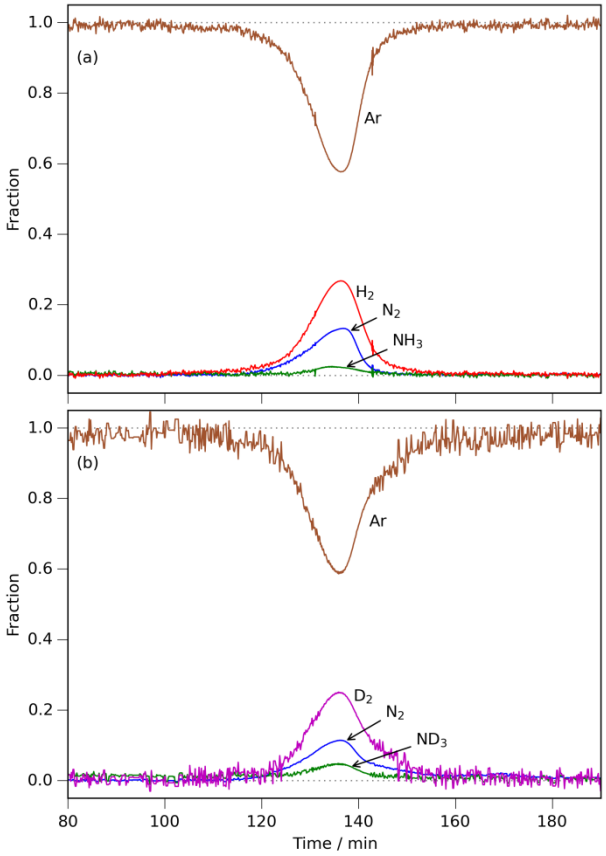

Figure 5: Decomposition of (a) $NaNH_2$ and (b) $NaND_2$ under flowing argon.

The stark difference between the decompositions of sodium amide and its deuterated analogue under argon and under ammonia indicates that two different mechanisms must be in operation depending on the composition of the surrounding gas. The bonds which are broken and formed in the $NaNH_2$ decomposition are four N-H bond scissions, two H-H bond formations and one N≡N bond formation (see equation (9)). Given that no kinetic isotope effect is observed for the amide decomposition under argon, the rate-limiting step in that reaction cannot involve N-H bond scission or H-H bond formation, which leaves N≡N bond formation as the only possibility. This also indicates that (i) the amide decomposition reaction under flowing argon proceeds *via* more than one step (since a single-step reaction would necessitate some N-H scission or H-H bond formation, see equation (9)) and (ii) there must be an intermediate species of nitrogen chemisorbed onto the sodium/sodium amide. These considerations leave two possible reaction pathways for the decomposition of the sodium amide under flowing argon. Firstly:

$$NaNH_2 \rightleftharpoons Na\text{-}N + H_2 \qquad (12)$$

$$2(Na\text{-}N) \rightarrow 2Na + N_2 \qquad (13)$$

Secondly:

$$2NaNH_2 \rightleftharpoons 2(Na\text{-}NH) + H_2 \quad (14)$$

$$2(Na\text{-}NH) \rightleftharpoons 2(Na\text{-}N) + H_2 \quad (15)$$

$$2(Na\text{-}N) \rightarrow 2Na + N_2 \quad (16)$$

Given that the evolution of hydrogen occurs at around the same time as the evolution of nitrogen for the amide decomposition under flowing argon, this would indicate that the reverse reaction of equation (12) (or those of equations (14) and (15)) has a large rate constant (relative to the forward reaction) as is the case with the transition metal-mediated ammonia decomposition reaction.[17]

For the decomposition under argon, both nitrogen atoms in the N_2 product must come from the amide itself (since there is no other source). By contrast, the decomposition of amide in the presence of ammonia has two potential sources of nitrogen for the N_2 product, sodium amide itself and ammonia. Since there is a significant kinetic isotope effect in the presence of ammonia (k_H/k_D = 1.77(11)), and, for $NaNH_2$, the amide decomposition reaction does not include the rate-limiting step, there is an implied necessity of the presence of an NH_3 molecule in the N_2 formation step for $NaNH_2$ under NH_3. This also indicates that the $NaNH_2$ mediated NH_3 decomposition reaction cannot be simply dichotomized into the two steps of formation and decomposition of the amide (equations (8) and (9)). For $NaND_2$, however, the amide decomposition does include the rate-limiting step (as shown by the sodium existing as amide not sodium metal), therefore it could proceed *via* either mechanism present in the $NaNH_2$ plus NH_3 or the $NaNH_2$ plus argon cases.

Bulk Catalyst Effect on Ammonia Decomposition

The final question for the sodium amide-mediated ammonia decomposition reaction is whether, as previously postulated,[5] the entire catalyst powder is involved in the reaction, or, as in the case for transition metal catalysts, only surface sites are active. Looking at the mass spectrometry data for the two ammonia decomposition reactions presented, it is clear that the change from NH_3 to ND_3 (defined by the deuteration fraction of ammonia, "$ND_3/(NH_3+ND_3)$") in the $NaNH_2$ experiment is much quicker than the ND_3 to NH_3 change for $NaND_2$, Figure 4. This is confirmed by inspection of the total volumes of gas that are released, Table 1, with "ND_3" (and its partially deuterated isotopologues) being the predominant part of the D released from the $NaND_2$ catalyst and residual gas within the reactor. This correlates with the fact that H-D exchange occurs rapidly at 300 °C when flowing ND_3 over $NaNH_2$ (which is how the $NaND_2$ for the reactions presented was synthesised) or NH_3 over $NaND_2$, whereas ammonia decomposition only starts occurring above 400 °C. Thus, in the $NaND_2$ experiment, after switchover to NH_3, any $NaND_2$ available is subject to rapid H-D exchange with any NH_3 molecules present. This reaction proceeds much more rapidly than the decomposition,

hence ND_3 is the predominant volume component of D released. Conversely, for the $NaNH_2$ plus ND_3 experiment, there is very little amide (the catalyst existing as almost entirely sodium), therefore there is minimal H-D exchange between $NaNH_2$ and ND_3, leaving H_2 as the predominant volume component of H released. Given this, it is pertinent to note that for the $NaND_2$ plus NH_3 experiment, the fraction of ammonia ("NH_3+ND_3", directly related to the conversion) displays a similar decay shape to that of the deuteration fraction of the ammonia, "ND_3/(NH_3+ND_3)", as shown in the normalized plot of Figure 6 (both are fitted to double exponential decays). This indicates that the more the $NaND_2$ exchanges its deuterium for hydrogen from NH_3 (along with ensuing amide decomposition to shift the equilibrium towards sodium rather than sodium amide), the greater the conversion, therefore the chemical composition of the whole of the catalyst affects the kinetics of the ammonia decomposition reaction. For the $NaNH_2$ plus ND_3 experiment, the "NH_3+ND_3" and the "ND_3/(NH_3+ND_3)" fraction change relatively quickly, because, as outlined above, the amide exists as mostly sodium metal.

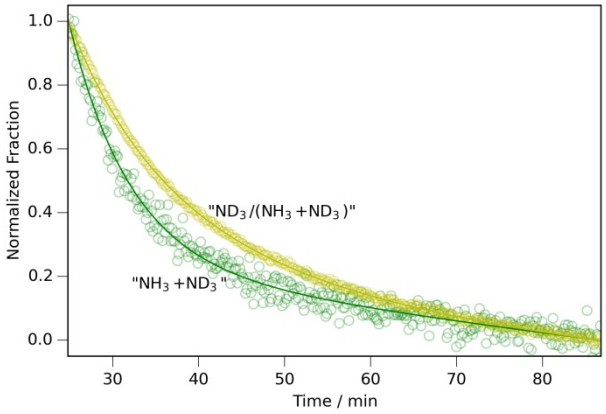

Figure 6: Normalized plot of the fraction of ammonia versus the deuteration fraction of that ammonia for the $NaND_2$ experiment after switchover from ND_3 to NH_3. Both lines are fitted double exponential decays. This is from the data presented in Figure 4(b).

For both the $NaNH_2$ and $NaND_2$ experiments, the change from H_2 to D_2 (and vice versa in the $NaND_2$ experiment) is on a similar timescale (allowing for the small delay in $NaNH_2$ experiment due to the ND_3 reaction with the sodium metal) and the volumes of HD produced are similar (allowing for different conversions). This suggests that the formation of H_2 or D_2 is happening on or close to the surface of the sodium/sodium amide catalyst. This contrast to the time taken for ND_3 to change to NH_3 for the $NaND_2$ experiment is consistent with the kinetics of ammonia decomposition being closely related to the availability of surface sodium sites, *i.e.* that the ammonia decomposition is effected on the surface of the catalyst, but the composition of the bulk of the catalyst affects the concentration of active surface sites.

Conclusions

The existence of a significant kinetic isotope effect when sodium amide is present (k_H/k_D = 1.77(11)) contrasted to its absence for the blank reactor (k_H/k_D = 1.10(8)) confirms that sodium amide decomposes ammonia *via* a different mechanism to that of nickel (and therefore other transition metals) and that it cannot be acting merely as a promoter for the latter. The presence of a kinetic isotope effect also indicates that $NaNH_2$ decomposition proceeds by a different reaction mechanism under NH_3 to under argon, where a kinetic isotope effect is absent. The favouring of the sodium amide formation or decomposition reactions is related to the partial pressure of ammonia within the reactor. The close relationship between the deuteration fraction of ammonia species exchanging with the $NaND_2$ and the ammonia conversion fraction indicates that the chemical nature of the entire catalyst, not just of a few active sites, affects the ammonia decomposition reaction.

ASSOCIATED CONTENT

Electronic Supporting Information (ESI)

Data fitting procedures, Raman spectra of $NaNH_2$ and $NaND_2$, infrared data.

AUTHOR INFORMATION

Corresponding Author

bill.david@stfc.ac.uk

Funding Sources

This work was financially supported by an STFC Innovations Proof of Concept Award (Phase 3 POCF1213-14) and an STFC CLASP Award (ST/L006278/1).

Notes

The authors declare no competing financial interest

Acknowledgments

The authors acknowledge the technical assistance of Mark Kibble and James Taylor for experimental support and laboratory management, and Kate Ronayne and Beth Evans for project management and useful guidance.

REFERENCES

(1) L. Green Jr., An ammonia energy vector for the hydrogen economy, *Int. J. Hydrogen Energy*, 1982, **7**, 355–359.

(2) W. Avery, A role for ammonia in the hydrogen economy, *Int. J. Hydrogen Energy*, 1988, **13**, 761–773.

(3) W. I. F. David, Effective hydrogen storage: a strategic chemistry challenge, *Faraday Discuss.*, 2011, **151**, 399–414.

(4) S. Orimo, Y. Nakamori, J. R. Eliseo, A. Züttel and C. M. Jensen, Complex Hydrides for Hydrogen Storage, *Chem. Rev.*, 2007, **107**, 4111–4132.

(5) W. I. F. David, J. W. Makepeace, S. K. Callear, H. M. A. Hunter, J. D. Taylor, T. J. Wood and M. O. Jones, Hydrogen Production from Ammonia using Sodium Amide, *J. Am. Chem. Soc.*, 2014, **136**, 13082–13085.

(6) A. W. Titherley, Sodium, Potassium, and Lithium Amides, *J. Chem. Soc.*, 1894, **65**, 504–522.

(7) D. A. Hansgen, D. G. Vlachos and J. G. Chen, Using first principles to predict bimetallic catalysts for the ammonia decomposition reaction, *Nat. Chem.*, 2010, **2**, 484–489.

(8) J. C. Ganley, F. S. Thomas, E. G. Seebauer and R. I. Masel, A Priori Catalytic Activity Correlations: The Difficult Case of Hydrogen Production from Ammonia, *Catal. Lett.*, 2004, **96**, 117–122.

(9) K. S. Love and P. H. Emmett, The Catalytic Decomposition of Ammonia over Iron Synthetic Ammonia Catalysts, *J. Am. Chem. Soc.*, 1941, **63**, 3297–3308.

(10) W. Tsai and W. H. Weinberg, Steady-state decomposition of ammonia on the ruthenium(001) surface, *J. Phys. Chem.*, 1987, **91**, 5302–5307.

(11) S. R. Logan, R. L. Moss and C. Kemball, The catalytic decomposition of ammonia on evaporated iron films, *Trans. Faraday Soc.*, 1958, **54**, 922–930.

(12) G. Ertl and M. Huber, Mechanism and kinetics of ammonia decomposition on iron, *J. Catal.*, 1980, **61**, 537–539

(13) S. R. Logan and C. Kemball, The catalytic decomposition of ammonia on evaporated metal films, *Trans. Faraday Soc.*, 1960, **56**, 144–153.

(14) N. Takezawa and I. Toyoshima, The Change of the Rate-Determining Step of the Ammonia Decomposition over an Ammonia Synthetic Iron Catalyst, *J. Phys. Chem.*, 1966, **70**, 594–595.

(15) H. Shindo, C. Egawa, T. Onishi and K. Tamaru, Reaction Mechanism of Ammonia Decomposition on Tungsten, *J. Chem. Soc., Faraday Trans.*, *1* 1980, **76**, 280–290.

(16) J. J. Vajo, W. Tsai and W. H. Weinberg, Mechanistic details of the heterogeneous decomposition of ammonia on platinum, *J. Phys. Chem.*, 1985, **89**, 3243–3251.

(17) K. Tamaru, A “new” general mechanism of ammonia synthesis and decomposition on transition metals, *Acc. Chem. Res.*, 1988, **21**, 88–94.

(18) K. S. Love and S. Brunauer, The Effect of Alkali Promoter Concentration on the Decomposition of Ammonia Over Doubly Promoted Iron Catalysts, *J. Am. Chem. Soc.*, 1942, **64**, 745–751.

(19) W. Raróg, Z. Kowalczyk, J. Sentek, D. Składanowski, D. Szmigiel and J. Zieliński, Decomposition of ammonia over potassium promoted ruthenium catalyst supported on carbon, *Appl. Catal. A*, 2001, **208**, 213–216.

(20) W. Raróg-Pilecka, D. Szmigiel, Z. Kowalczyk, S. Jodzis and J. Zielinski, Ammonia decomposition over the carbon-based ruthenium catalyst promoted with barium or cesium, *J. Catal.*, 2003, **218**, 465–469.

(21) S. F. Yin, B. Q. Xu, X. P. Zhou and C. T. Au, A mini-review on ammonia decomposition catalysts for on-site generation of hydrogen for fuel cell applications, *Appl. Catal. A*, 2004, **277**, 1–9.

(22) R. Z. Sørensen, L. J. E. Nielsen, S. Jensen, O. Hansen, T. Johannessen, U. Quaade and C. H. Christensen, Catalytic ammonia decomposition: miniaturized production of CO_x-free hydrogen for fuel cells, *Catal. Commun.*, 2005, **6**, 229–232.

(23) K. Kiełbasa, R. Pelka and W. Arabczyk, Studies of the Kinetics of Ammonia Decomposition on Promoted Nanocrystalline Iron Using Gas Phases of Different Nitriding Degree, *J. Phys. Chem. A*, 2010, **114**, 4531–4534.

(24) J. W. Makepeace, T. J. Wood, H. M. A. Hunter, M. O. Jones and W. I. F. David, Ammonia decomposition catalysis using non-stoichiometric lithium imide, *Chem. Sci.*, 2015, DOI: 10.1039/C5SC00205B.

(25) F. H. Westheimer, The Magnitude of the Primary Kinetic Isotope Effect for Compounds of Hydrogen and Deuterium, *Chem. Rev.*, 1961, **61**, 265–273.

(26) R. A. van Santen, Chemical basis of metal catalyst promotion, *Surf. Sci.*, 1991, **251–252**, 6–11.

(27) G. Ertl, S. B. Lee and M. Weiss, Adsorption of nitrogen on potassium promoted Fe(111) and (100) surfaces, *Surf. Sci.*, 1982, **114**, 527–545.

(28) S. Brunauer, K. S. Love and R. G. Keenan, Adsorption of Nitrogen and the Mechanism of Ammonia Decomposition Over Iron Catalysts, *J. Am. Chem. Soc.*, 1942, **64**, 751–758.

(29) N. Takezawa and I. Toyoshima, The Change of the Rate-Determining Step of the Ammonia Decomposition over an Ammonia Synthetic Iron Catalyst, *J. Phys. Chem.*, 1966, **70**, 594–595.

(30) N. Takezawa and I. Toyoshima, The Rate-determining Step of Ammonia Decomposition over a Well-reduced Doubly Promoted Iron Catalyst, *J. Res. Inst. Catalysis, Hokkaido Univ.*, 1966, **14**, 41–58.